JAK/STAT Signaling Governs Airway Epithelial Homeostasis and Stress Resilience in *Drosophila*

Xiao Niu[1, 2], Christine Fink[1], Kimberley Kallsen[3, 4], Leizhi Shi[1, 5], Viktoria Mincheva[1], Sören Franzenburg[6], Ruben Prange[1], Iris Bruchhaus[7], Holger Heine[2, 8], Judith Bossen[1, 8*], Thomas Roeder[1, 8*]

[1]Kiel University, Zoology, Dept. of Molecular Physiology, Kiel, Germany

[2]Current address: Weifang Medical University, College of Life Science and Technology, Weifang, China

[3]Research Center Borstel – Leibniz Lung Center, Div. of Innate Immunity, Borstel, Germany

[4]Current address: Boehringer Ingelheim, Ingelheim, Germany

[5]Department of Thoracic Surgery, Linyi People's Hospital, Linyi, Shandong, 276000, China

[6]Kiel University, IKMB, Kiel, Germany

[7]Bernhard Nocht Institute for Tropical Medicine, Hamburg, Germany

[8]German Center for Lung Research, Airway Research Center North, Kiel, Germany

*Correspondence: Judith Bossen, email: jbossen@zoologie.uni-kiel.de; Thomas Roeder, email: troeder@zoologie.uni-kiel.de

Highlights

1. JAK/STAT signaling is active throughout the entire *Drosophila* respiratory system during all developmental stages.
2. The signaling pathway is indispensable for the survival of the tracheal cell.
3. Overactivation of the signaling profoundly impacts tracheal development and exhibits a phenotype associated with human diseases in the *Drosophila* trachea.

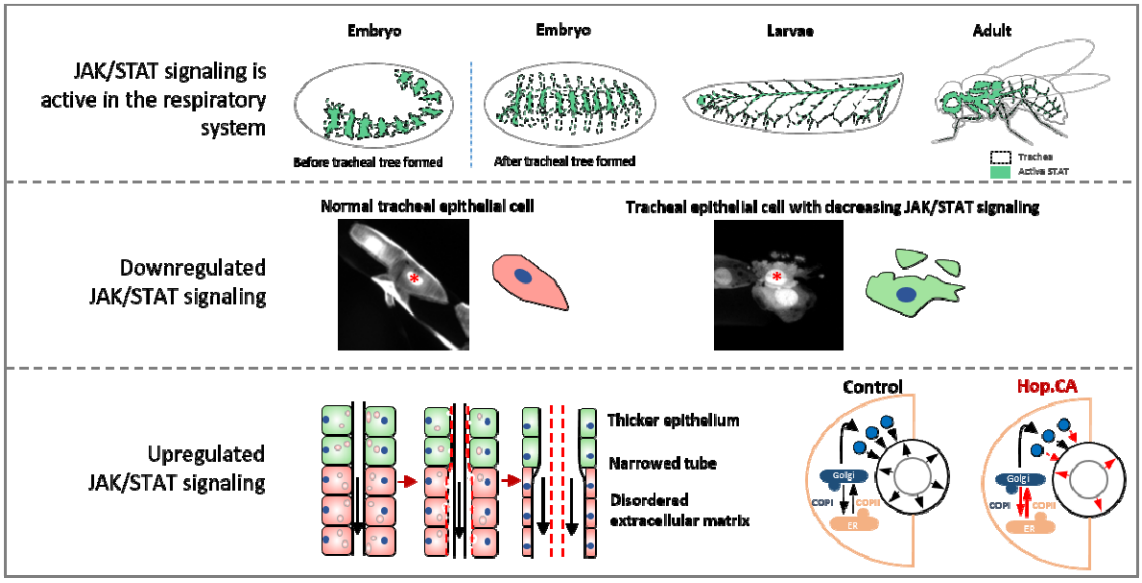

Summary

Respiratory epithelial cells must dynamically adapt to continuous environmental challenges, yet the molecular pathways that govern their stress responses remain incompletely understood. This study demonstrates that the JAK/STAT signaling pathway is a crucial regulator of airway epithelial cell survival and homeostasis in *Drosophila melanogaster*. Our findings reveal that JAK/STAT activity is continuously required throughout development and adulthood, with environmental factors like cigarette smoke and hypoxia further intensifying pathway activation. Disrupting JAK/STAT signaling in airway epithelia during development is lethal, triggers apoptosis, and in adults, reduces lifespan while increasing vulnerability to chronic smoke exposure. Conversely, chronic hyperactivation of JAK/STAT signaling induces significant cell-autonomous epithelial remodeling, evidenced by epithelial thickening, tracheal narrowing, and impaired barrier structure, mirroring the pathological features of chronic lung disease. Pharmacological inhibition of this pathway effectively reverses these defects. Comprehensive transcriptomic analyses further reveal that maintaining a balance in JAK/STAT signaling is essential for preserving cellular junctions and secretory functions. These findings underscore the importance of tightly regulated JAK/STAT signaling for the integrity of airway epithelium and present a valuable in vivo model for exploring the mechanisms underlying inflammatory lung diseases and for preclinical drug testing.

Introduction

The respiratory epithelium is a dynamic barrier that interfaces directly with the external environment, orchestrating both defense and repair mechanisms essential for pulmonary homeostasis (Whitsett & Alenghat, 2015). These cells are persistently exposed to environmental stressors, airborne pathogens, and inflammatory signals, necessitating highly adaptive intracellular signaling to maintain tissue integrity and immune balance (Hewitt & Lloyd, 2021). Among the core pathways mediating this responsiveness, the Janus kinase/signal transducer and activator of transcription (JAK/STAT) signaling axis emerges as a pivotal regulator of epithelial function (Hu *et al*, 2021; Villarino *et al*, 2017).

The JAK/STAT pathway directly links extracellular signals to nuclear transcriptional programs, influencing processes that range from development to inflammation resolution (Kiu & Nicholson, 2012). Notably, almost every cell type in the lung, including airway epithelial cells, is modulated by cytokine signaling through JAK/STAT (Villarino *et al.*, 2017; Yew-Booth *et al*, 2015). Dysregulated pathway activity is increasingly recognized as a hallmark of several chronic lung diseases, including asthma, chronic obstructive pulmonary disease (COPD), idiopathic pulmonary fibrosis (IPF), and lung cancer (Dutta *et al*, 2014; Georas *et al*, 2021; Milara *et al*, 2018; Yew-Booth *et al.*, 2015). While diminished signaling impairs epithelial regeneration and defense (Tadokoro *et al*, 2014b), hyperactivation contributes to persistent inflammation and tissue remodeling (Jin *et al*, 2018; Major *et al*, 2020; Makris *et al*, 2017).

Despite its essential role and its simple general architecture, the vertebrate JAK/STAT signaling system is highly complex, characterized by multiple ligands, receptors, and transcription factors that often display functional redundancy and cell-type specificity (Hu *et al.*, 2021; Morris *et al*, 2018; Villarino *et al.*, 2017). This complexity has impeded precise dissection of pathway dynamics in specific cell

populations such as airway epithelial cells. To overcome this limitation, genetically tractable model systems with reduced signaling complexity offer a promising strategy.

Drosophila melanogaster presents a streamlined model for investigating JAK/STAT signaling, featuring only one receptor (Domeless), one Janus kinase (Hopscotch), and one STAT transcription factor (STAT92E) (Arbouzova & Zeidler, 2006; Zeidler & Bausek, 2013). Coupled with its powerful genetic toolkit and well-characterized airway-like tracheal system, *Drosophila* enables direct and targeted interrogation of epithelial-specific signaling processes (Bossen *et al*, 2021; Levine & Cagan, 2016; Pandey & Nichols, 2011; Prange *et al*, 2018; Roeder *et al*, 2009; Roeder *et al*, 2012). While prior studies have elucidated JAK/STAT functions in early tracheal development (Brown *et al*, 2001; Perrimon & Mahowald, 1986; Powers & Srivastava, 2019), the role of this pathway in mature airway epithelia under homeostatic or stress conditions remains poorly defined.

A lack of JAK/STAT signaling during very early phases of tracheal development impairs tracheal development including cell movement and elongation, as well as invagination processes that lead to tube formation (Brown *et al.*, 2001; Isaac & Andrew, 1996). During the development of the vertebrate lung, very similar processes are operative (Nogueira-Silva *et al*, 2006; Piairo *et al*, 2018).

In this study, we leverage the simplicity of the *Drosophila* model to systematically dissect the functional relevance of JAK/STAT signaling in airway epithelial cells. By experimentally manipulating the pathway within this defined cellular context, we uncover how deregulation impacts epithelial integrity and contributes to pathological remodeling. Our findings shed light on conserved mechanisms of epithelial regulation and provide a foundation for understanding how aberrant JAK/STAT activity may drive human chronic lung disease pathogenesis.

Results

JAK/STAT Signaling in Airway Epithelia Responds Rapidly to Environmental Stressors

To explore the responsiveness of airway epithelial cells to external stress via the JAK/STAT pathway, we employed a *STAT92E*-dependent GFP reporter system in *Drosophila* (Bach *et al*, 2007). Upon exposure to airborne stressors, including cold air, hypoxia, and cigarette smoke exposure (CSE), both larvae and adults exhibited robust upregulation of reporter activity in airway epithelial cells (Fig. 1A, 1C). Quantitative fluorescence analysis confirmed statistically significant induction of JAK/STAT signaling under all stress conditions (Fig. 1A′, 1C′). Significantly, this activation spatially overlapped with enhanced expression of the cytokine *upd3*, a key JAK/STAT ligand. While *upd2* was selectively induced by CSE, *upd3* was responsive to all tested stressors in both larvae and adults (Fig. 1B, B′, 1D, D′, Fig. S1). These results demonstrate that external stimuli dynamically modulate ligand expression and downstream pathway activation in the airway epithelium.

Spatial Dynamics Reveal JAK/STAT Activity in Regenerative Zones of the Tracheal System

Under steady-state conditions, the JAK/STAT pathway was active in distinct regions of the larval trachea. These regions comprise the almost entire dorsal trunks and primary branches of the larval trachea (Fig. 2A). Minimal reporter activity was observed in Tr10, a region undergoing apoptosis during

metamorphosis (Fig. 2B) (Bosch *et al*, 2015; Chen & Krasnow, 2014). Reporter activity was particularly pronounced in the spiracular branch (SB), dorsal branch (DB), and tracheal metamere Tr2, all areas associated with epithelial cell proliferation and repair (Guha *et al*, 2008; Sato *et al*, 2008; Weaver & Krasnow, 2008) (Fig. 2C–D).

In adult tracheae, the pathway remained active across epithelial cells throughout the respiratory network (Fig. 2E), underscoring its role beyond development. Enhancer-driven reporter analysis confirmed significant *upd2* expression in the tracheal system, especially in the Tr2 and Tr10 regions as well as in the SB tracheoblasts (Fig. S2C), showing that the airway epithelium is both a sender and a responder of this pathway. This confirms that JAK/STAT signaling is intrinsically linked to airway epithelial function.

JAK/STAT Signaling Is Essential for Tracheal Integrity and Organismal Viability

We inhibited JAK/STAT activity in tracheal epithelial cells to assess pathway necessity by expressing a dominant-negative Domeless (*Dome.DN*) receptor allele. Temporal control using the TARGET system (McGuire *et al*, 2004) revealed early embryonic inhibition led to lethality during larval development (Fig. 3A, Fig. S3).

Microscopy revealed profound tracheal defects: loss of the dorsal trunk (DT), segmental fusion, and apoptotic cell death in a cell-autonomous fashion (Fig. 3B–C). Caspase-1 (Dcp-1) staining confirmed apoptosis specifically in *Dome.DN*-expressing epithelial cells (Fig. 3D–F). Thus, basal JAK/STAT activity is indispensable for maintaining tracheal architecture and epithelial survival.

In adults, trachea-specific inhibition significantly shortened lifespan and reduced tolerance to chronic CSE exposure (Fig. 3G), though it did not affect responses to hypoxia (Fig. 3H–I), indicating a stress-specific requirement for the pathway.

Hyperactivation of JAK/STAT Causes Lethality and Cell-Autonomous Epithelial Remodeling

To test the consequences of excessive pathway activity, we overexpressed *Hop.CA* (constitutively active JAK) and *upd3* in the trachea. Both interventions resulted in embryonic or early larval death (Fig. 4A–B), with *upd3*-overexpressing embryos that survived displaying more severe structural defects than those overexpressing *Hop.CA* (Fig. 4C–E″).

Those larvae that survived the hyperactivation of JAK/STAT signaling using the inducible TARGET system (McGuire *et al.*, 2004) displayed dramatic epithelial thickening, which required at least 48 hours of ectopic activation (Fig. 4F, Fig. S4). Mosaic analysis confirmed that this phenotype was cell-autonomous, affecting only *Hop.CA*-expressing cells (Fig. 4G). The increased thickness depended on cell volume expansion rather than an increase in cell number (Fig. 4H–K), as clarified by concurrent quantification of epithelial thickness (Fig. 4H, I), length (Fig. 4H, J), and cell number (Fig. 4K).

Weaker expression drivers (e.g., *nach*-Gal4) that lead to weaker JAK/STAT activation produced the phenotype with reduced severity (Fig. 4L–M). The expression of *Dome.DN* in the trachea caused liquid accumulation and larval death, confirming an impaired epithelial barrier function (Fig. 4O). We further demonstrated that the epithelial thickening phenotype caused by hyperactivation of JAK/STAT signaling is independent of another intervention that induced this phenotype, the ectopic activation of the IMD pathway (Fig. 4P).

Transcriptomic Profiling Links Chronic JAK/STAT Activation to Innate Immunity and Transport Dysfunction

RNA-seq analysis of tracheal cells expressing *Hop.CA* revealed 2,004 differentially expressed genes (DEGs), 876 of which were upregulated (Table 1) and 1,128 downregulated (Fig. S5). Principal component analysis cleanly separated experimental and control groups, and expression of canonical targets (*Hop*, *Socs36E*) validated pathway activation (Fig. S5B).

Functional enrichment analysis (KEGG, GO) revealed: A) Upregulation of genes in innate immunity (e.g., multiple antimicrobial peptide genes including those of the Bomanin family (Lindsay *et al*, 2018)) and vesicle-mediated transport (Fig. 5A–B). B) Downregulation of genes involved in cuticle and epicuticle development. There is altered expression in pathways related to RNA processing, muscle differentiation, and chemical detection (Table S1). A promoter scan analysis indicated that not all strongly upregulated genes are direct targets of the JAK/STAT signaling pathway (Table 2).

Strikingly, the immune activation and vesicle transport signature observed in the *Drosophila* trachea mirrored the changes seen in a murine asthma model (Fig. 5C-F). Airway structural remodeling was also evident (Fig. 5C–D). A substantial increase in the transcript levels of cytokines and cytokine receptors (Fig. 5E), key players in the pro-inflammatory network that operates via the JAK/STAT pathway, aligns with the role of the JAK/STAT pathway in *Drosophila* airway epithelia. This is also evident in the altered transcript levels of genes involved in vesicular transport (Fig. 5F), emphasizing the conserved role of JAK/STAT hyperactivation in airway disease.

Pharmacological Inhibition of JAK/STAT Ameliorates Epithelial Remodeling

To assess this study's translational potential, we treated *Hop.CA*-expressing animals with clinically approved JAK inhibitors (Fig. 5G, H). All three tested compounds—Baricitinib, Oclacitinib, and Filgotinib—reduced epithelial thickening by over 60%, highlighting the suitability of *Drosophila* as a drug screening platform for airway-targeted therapeutics (Fig. 5G, H).

Chronic JAK/STAT Activation Disrupts Protein Transport and Tracheal Architecture

To evaluate if the transport capacities in the *Drosophila* airway epithelial cells are impaired, we focused on two peripheral membrane-associated proteins involved in cell-cell interactions. Coracle (Cora), a component of the septate junctions, and Armadillo (Arm), a component of the adherens junctions, depend on vesicle transport to reach their final destinations (Lock & Stow, 2005; Oshima & Fehon, 2011) (Fig. 6A). Immunostaining of mosaic animals revealed cytoplasmic retention of Arm (Fig. 6B, C) and Cora (Fig. 6D, E) only in *Hop. CA*-expressing cells, consistent with defective vesicle trafficking.

Correspondingly, chitinous taenidia, critical for tracheal stability (Glasheen *et al*, 2010), were malformed or absent in *Hop.CA* overexpressing animals (Fig. 7A–B″), indicating structural failure of the airway epithelium. Mosaic animals further demonstrated that tracheal disorganization was spatially restricted to areas expressing *Hop.CA* (Fig. 7C, D). Moreover, we only observed a narrowing of the air conducting lumen in these regions (Fig. 7C, D). These phenotypes support a model in which JAK/STAT overactivation impairs vesicle-mediated transport, limiting delivery of junctional components and structural proteins, which is in line

with previous findings about this biological process (Jayaram *et al*, 2008; Tsarouhas *et al*, 2007)(Fig. 7E). Severe lumen narrowing observed in high-expression zones underscores the physiological relevance of these structural defects.

Together, these findings establish JAK/STAT signaling as a central regulator of airway epithelial homeostasis. Its dysregulation drives profound morphological, transcriptional, and functional changes that parallel chronic respiratory diseases, and can be pharmacologically modulated in a genetically tractable *Drosophila* model.

Discussion

Drosophila Enables Dissection of Core JAK/STAT Functions in the Airway Epithelium

In this study, we used *Drosophila melanogaster* to dissect the fundamental roles of the JAK/STAT pathway in respiratory epithelial cells. The fruit fly presents a uniquely advantageous model: its minimal JAK/STAT architecture, comprising one receptor (Domeless), one JAK (Hopscotch), and one STAT (STAT92E), eliminates the complexities of mammalian redundancy, allowing clean genetic manipulation of the entire signaling cascade. Our major findings demonstrate that: A) JAK/STAT signaling is constitutively active in airway epithelia across developmental stages; B) Environmental stressors, such as hypoxia and cigarette smoke, robustly enhance pathway activity; C) Pathway inhibition leads to epithelial apoptosis, while ectopic activation results in structural remodeling resembling human chronic lung disease. These results collectively position

JAK/STAT signaling as a central regulator of airway epithelial cell survival, stress responsiveness, and structural integrity.

JAK/STAT Signaling Balances Survival and Stress Response in the Epithelium

The tonic activity of JAK/STAT signaling observed during embryonic, larval, and adult stages supports a baseline survival function. Pathway inhibition through dominant-negative Domeless induced widespread apoptosis, aligning with previous findings in mammalian epithelial systems (Quinton & Mizgerd, 2011; Zheng *et al*, 2016). This underscores a conserved cytoprotective role, likely mediated by the cytokine ligands Upd2 and Upd3, which act organ-autonomously.

Upon stress exposure, such as cigarette smoke or hypoxia, JAK/STAT activity is further amplified, mirroring protective responses seen in mammalian airway epithelia (Kida *et al*, 2008; Paris *et al*, 2020; Tadokoro *et al*, 2014a) (Hokuto *et al*, 2004). This aligns with findings from *Drosophila* intestinal models, where epithelial stress triggers Upd3 expression, which activates stem cells (Jiang *et al*, 2009; Miguel-Aliaga *et al*, 2018). Although the trachea lacks stem cell-mediated regeneration, this stress-activated signaling system operates in this tissue. These data point to a dual role for JAK/STAT signaling in maintaining airway epithelial homeostasis and coordinating emergency responses to environmental insults.

Hyperactivation Mirrors Pathology of Chronic Lung Disease

While a threshold level of signaling is protective, sustained or excessive JAK/STAT activity drove phenotypes akin to asthma, COPD, pulmonary fibrosis, and lung cancer (Adnot *et al*, 2019; Chen *et al*, 2021; D'Amico *et al*, 2018; Dutta

et al., 2014; Gao *et al*, 2004; Milara *et al.*, 2018; Parakh *et al*, 2021; Prele *et al*, 2012; Simeone-Penney *et al*, 2007; Yew-Booth *et al.*, 2015; Zhang *et al*, 2012). Tracheal remodeling, including epithelial thickening, luminal narrowing, and disrupted extracellular matrix, was cell-autonomous and time-dependent, revealing how chronic activation directly reshapes epithelial architecture.

These changes resemble epithelial-to-mesenchymal transition (EMT), a process dependent on JAK/STAT activity in lung cancer (Liu *et al*, 2014). Furthermore, transcriptomic analyses revealed widespread immune and secretory gene alterations, including the upregulation of Bomanin antimicrobial peptides, paralleling immune shifts in diseased mammalian airways (Choi *et al*, 2013; Simeone-Penney *et al.*, 2007).

However, this activation came at a cost: vesicle transport was impaired, junctional proteins like Coracle and Armadillo were mislocalized, and barrier function was compromised, phenotypes typical of barrier breakdown in chronic lung disease (Georas & Rezaee, 2014; Gon & Hashimoto, 2018; Heijink *et al*, 2012). These findings support the hypothesis that chronic JAK/STAT activation contributes to airway dysfunction, rather than repair.

Developmental Roles Are Conserved but Context-Specific

Our study also refined the role of JAK/STAT signaling in tracheal development, particularly in dorsal trunk formation. While prior literature questioned the necessity of this pathway in mammalian lung development (Tadokoro *et al.*, 2014a), emerging data suggest otherwise (Piairo *et al.*, 2018). In *Drosophila*, we confirmed that the pathway is essential across embryonic, larval, and adult stages, with its disruption leading to failure in tracheal tube patterning and

function. This highlights its developmental importance, even if contextual differences exist between invertebrate and vertebrate systems.

Drosophila **as a Preclinical Model for Respiratory Disease and Drug Screening**

Beyond mechanistic insight, our data establish *Drosophila* as a functional model for chronic airway disease. The transcriptomic and structural hallmarks observed upon JAK/STAT hyperactivation mirrored those found in a murine asthma model, suggesting high interspecies relevance. Most notably, treatment of affected flies with clinically relevant JAK inhibitors (Baricitinib, Oclacitinib, Filgotinib) significantly reversed epithelial thickening and rescued viability. This pharmacological rescue highlights the fly's utility as a drug screening platform, allowing rapid and tractable testing of airway-targeted interventions.

The predictability and cell-specificity of phenotypes in *Drosophila* also underscore the relevance of airway epithelial cells as the primary therapeutic target, reinforcing inhalation as a rational route for delivery in humans.

Evolutionary Considerations and Model Value

Although the insect trachea and vertebrate lung are not homologous, both share key features in epithelial architecture, immune signaling, and environmental exposure (ANDREW AND EWALD 2010; BERGMAN *et al.* 2017). This partial conservation validates the fly trachea as a proxy for mechanistic studies of epithelial homeostasis and pathogenesis in the respiratory tract (Bossen *et al*, 2019; Kallsen *et al*, 2015; Levine & Cagan, 2016; Prange *et al.*, 2018; Roeder *et al.*, 2009; Roeder *et al.*, 2012) .

Given its simplicity, genetic accessibility, and capacity for real-time in vivo monitoring, the *Drosophila* model represents a powerful experimental system to investigate airway epithelial biology and test therapeutic hypotheses, particularly those targeting evolutionarily conserved pathways such as JAK/STAT,

Conclusion

Our study demonstrates that JAK/STAT signaling is essential but tightly regulated in respiratory epithelia. Its dysregulation induces molecular and structural pathologies resembling human airway diseases. The *Drosophila* model enables high-resolution analysis of these processes and provides a versatile platform for therapeutic discovery. As airway diseases continue to impose a global health burden, simplified and scalable systems like *Drosophila* offer strategic advantages for accelerating mechanistic insight and intervention design.

Materials and Methods

Drosophila strains and husbandry

STAT92E-GFP was used to monitor the pathway's activation (Bach *et al.*, 2007); the Gal4-UAS system (Brand & Perrimon, 1993) targeted ectopic expression to the tracheal system. The Gal4 drivers included: *btl-Gal4, UAS-GFP* on the 3rd chromosome, and *btl-Gal4, UAS-GFP* on the 2nd chromosome (obtained from the Leptin group, Heidelberg, Germany); *upd2-Gal4*; *upd3-Gal4 (Prange et al., 2018)*; *nach-Gal4 (Liu et al, 2003)*. The UAS responders consisted of: *UAS-LacZ.nls* (BDSC 3956), *UAS-domeΔcyt2.1* (*Dome.DN*), and *UAS-Hop.CA* (*UAS-hopTumL*), which were obtained from N. Perrimon (Brown *et al.*, 2001; Harrison *et al*, 1995). The *UAS-upd3* was constructed in our lab. *TubP-Gal80[ts]* (BDSC 7018) was obtained from the Bloomington stock center. Unless otherwise stated,

the flies were raised on standard medium at 25 °C with 50–60% relative humidity under a 12:12 h light/dark cycle as described earlier (Fink *et al*, 2016).

Coin-FLP expression system

Vvl-FLP/CyO; btl-moe.mRFP (BDSC 64233), *tubP-Gal80[ts]* and *CoinFLP-Gal4, UAS-2xEGFP* (BDSC 58751) were used to construct animals for the tracheal mosaic analysis. Ventral veins lacking (*vvl*) was expressed in larval tracheal clones that covered approximately 30 to 80% of the trachea (Bosch *et al.*, 2015; Chen & Krasnow, 2014). The genotype of the flies was *vvl-FLP*, *CoinFLP-Gal4*, *UAS-2xEGFP*/*CyO* (*vvl-coin*) and *vvl-FLP*, *CoinFLP-Gal4*, *UAS-2xEGFP*/*CyO*; *tub-Gal80[ts]* (*vvl-coin.ts*).

Developmental viability

For the developmental viability of eggs, they were collected overnight and not physically handled in any way. The number of hatched eggs and pupae were counted starting two days after collection. Each group had four replicates that included more than 20 eggs. Tub-Gal80 [ts] was used to limit UAS responder expression during the larval stage to study the developmental viability of larvae. Animals were raised at 18 °C to keep the UAS responder gene silent. Larvae at different instar stages were transferred to a new medium at 29 °C. In this study, four replicates were typically performed with 30 larvae each. The stage of the larvae was determined by the appearance of the anterior spiracles.

Determination of epithelial thickness

The L2 and L3 larvae trachea were carefully dissected from the posterior side of the body in PBS. The isolated trachea were immersed in 50% glycerol, and digital images were captured within 15 min. L2 larvae were distinguished from L3

larvae by the appearance of anterior spiracles. The relative ages of L3 larvae were inferred from the animal's size. Thirty larvae were used in each group, and specimens were analyzed by Image J.

Drug application in *Drosophila*

JAK inhibitors (Baricitinib #16707, Oclacitinib #18722, Filgotinib #17669 - Cayman Chemicals, Michigan, USA) were diluted in DMSO [100 mM]. For later application, the inhibitors were diluted 1:10 in 100% EtOH. We used 20 µl of each diluted inhibitor for 2 ml of concentrated medium (5% yeast extract, 5% corn flour, 5% sucrose, 1% low-melt agarose, 1 ml of 10% propionic acid, and 3 ml of 10% Nipagin). The eggs of each crossing have been applied to the modified medium and kept at 20 °C until the larvae reach the L2 stage. Afterwards, they were incubated at 30 °C for 2 days to induce the *btl-Gal4, UAS-GFP; tub-Gal80[ts]* (*btl.ts*)–driver. The trachea of L3 Larvae were carefully dissected from the posterior side of the body in PBS. The isolated trachea was immersed in 50% glycerol, and digital images were captured in 15 min. 10 larvae were used for each group.

Experimental design for hypersensitivity pneumonitis in mice

Experimental design for hypersensitivity pneumonitis contains two processes, sensitization and challenge of mice with ovalbumin (Sigma Aldrich, A5503). The protocol refers to the protocol that (Daubeuf & Frossard, 2013) is described with a few modifications. 8-week-old Balb/C mice were sensitized with intraperitoneal injections of 20 µg of OVA emulsified in aluminum hydroxide in a total volume of 1 ml on days 7 and 14, followed by three consecutive challenges each day by exposure to OVA or PBS aerosol for 30 min. Mice were sacrificed 24 h following the final challenge. The left lungs were collected for histological analysis, and the

superior lobes were dissected for RNA analysis. Six mice per group were used in this experiment and four mice were randomly selected in each group for analyses. Genesky performed total mRNA sequencing, data processing, and statistical analysis (Shanghai, China). The experimental protocols were approved by the Animal Care and Protection Committee of Weifang Medical University (2021SDL418).

AB-PAS staining and immunofluorescence analysis of mouse lung

Mice were sacrificed in an excess of CO_2 gas. The lungs of euthanized mice were inflated by intratracheal injection of cold 4% paraformaldehyde and then fixed and embedded in paraffin as described in (Baligar *et al*, 2016). AB-PAS staining and Immunofluorescence analysis were supported by Servicebio (Wuhan, China). All sections were photographed using a microscope slide scanner (Pannoramic MIDI: 3Dhistech). The materials and methods could be found at the following link https://www.servicebio.cn/data-detail?id=3040&code=MYYGSYBG and https://www.servicebio.cn/data-detail?id=35_95&code=RSSYBG. We list the primary reagents here: AB-PAS solution set (Servicebio, G1049), Anti-CD11b (Servicebio, GB11058), and DAPI (Servicebio, G1012-10ML).

Time-lapse microscopy

All images were acquired using a ZEISS Axio Image Z1 and a ZEISS LSM 880 fluorescent microscope (INST 257/591-1 FUGG). Embryos were dechorionated in 3% sodium hypochlorite and immersed in Halocarbon oil 700 (Sigma Aldrich, 9002-83-9, Deisenhofen, Germany). Then the embryos were imaged after stage 15 when the tracheal tree formed at 3-hour intervals. 40 embryos were investigated in each group.

Cigarette smoke and hypoxic exposure

All cigarette smoke exposure experiments were carried out in a smoking chamber, attached to a diaphragm pump. Common research 3R4F cigarettes (CTRP, Kentucky University, Lexington, USA) were used for all experiments. The vials containing animals were capped with a monitoring grid to allow the cigarette smoke to diffuse into the vial. For long-term smoke experiments, L2 larvae were exposed to smoke thrice a day for 30 minutes each, on two consecutive days. For heavy smoke experiments, L3 larvae were exposed to the smoke of 2 cigarettes for 45 min, which led to about 35-50% mortality. To study the effects of hypoxia on the activity of JAK/STAT signaling pathway, larvae were exposed to long-term and short-term hypoxia separately. For long-term hypoxia experiments, L2 larvae were exposed to 5% oxygen three times a day for 30 min each, on two consecutive days. L3 larvae were exposed to 1% oxygen once for 5 hours for short-term hypoxia experiments. At least 20 animals in 4 vials were investigated in each group. Cigarette smoke and hypoxia exposure of adults was performed as described earlier (Prange *et al.*, 2018)

Immunohistochemistry of *Drosophila* trachea

Larvae were dissected by ventral filleting and fixed in 4% paraformaldehyde for 30 min. Embryos were staged according to Campos-Ortega and Hartenstein (Campos-Ortega & Hartenstein, 1997) and fixed in 4% formaldehyde for 30 min. Immunostaining was performed following standard protocols as described earlier(Jeon *et al*, 2008; Levi *et al*, 2006). GFP signals were amplified by immunostaining with polyclonal rabbit anti-GFP (used at 1:500, Sigma-Aldrich, Merck KGaA, Darmstadt, Germany, SAB4301138). 40-1a (used at 1:50, DSHB, Iowa City, USA) was used to detect Beta-galactosidase. Coracle protein was detected with a monoclonal mouse anti-coracle antibody (used at 1:200, DSHB, Iowa City, USA, C566.9). Armadillo protein was detected with a monoclonal mouse anti-armadillo antibody (DSHB, US, N2 7A1, used at 1:500). A

monoclonal rabbit Cleaved Drosophila Dcp1 (used at 1:200, Cell Signaling, Frankfurt/M, Germany, #9578) was used to detect apoptotic cells. Secondary antibodies used were: Cy3-conjugated goat-anti-mouse, Cy3-conjugated goat-anti-rabbit, Alexa488-conjugated goat-anti-mouse (used at 1:500, Jackson Immunoresearch, Dianova, Hamburg, Germany), Alexa488-conjugated goat-anti-rabbit (used at 1:500, Cell signaling, Frankfurt/M, Germany, #9578). Tracheal chitin was stained with 505 star conjugated chitin-binding probe (NEB, Frankfurt/M, Germany, used at 1:300). Nuclei were stained with 4',6-Diamidino-2-Phenylindole, Dihydrochloride (DAPI) (Roth, Karlsruhe, Germany, 6843). 30 specimens were investigated in each group. Specimens were analyzed and digital images were captured either with a confocal (Zeiss LSM 880, Oberkochen, Germany) or a conventional fluorescence microscope (ZEISS Axio Imager Z1, Zeiss, Oberkochen, Germany), respectively.

RNA isolation and RNA sequencing

For the gene expression analysis of 3rd instar larvae trachea, animals were dissected in cold PBS and isolated trachea transferred to RNA Magic (BioBudget, Krefeld, Germany) and processed essentially as described earlier (Prange *et al.*, 2018) with slight modifications. The tissue was homogenized in a Bead Ruptor 24 (BioLab products, Bebensee, Germany) and the RNA was extracted by using the PureLink RNA Mini Kit (Thermo Fisher, Waltham, MA, USA) for phase separation with the RNA Magic reagent. An additional DNase treatment was performed following the on-column PureLink DNase treatment protocol (Thermo Fisher, Waltham, MA, USA).

Sequencing libraries were constructed using the TruSeq stranded mRNA kit (Illumina, San Diego, USA) and 50 bp single-read sequencing was performed on an Illumina HiSeq 4000 with 16 samples per lane. Resulting sequencing reads were trimmed for low-quality bases and adapters using the fastq Illumina filter

(http://cancan.cshl.edu/labmembers/gordon /fastq_illumina_filter/) and cutadapt (version 1.8.1)(Martin, 2011). Transcriptomics analysis, including gene expression values and differential expression analysis, was done using CLC Genomics Workbench. The detailed protocols can be obtained from the CLC Web site (http://www. clcbio.com/products/clc-genomics-workbench). *Drosophila melanogaster* reference genome (Release 6) (Hoskins *et al*, 2015) was used for mapping in this research.

The transcription factor binding site enrichment and the Gene Ontology enrichment analyses of the differentially expressed genes were carried out using Pscan (http://159.149.160.88/pscan/) and online GO enrichment analysis (http://geneontology. org/), respectively. We chose -450- 50 bases of the annotated transcription start site of the genes as the transcription factor binding sites for enrichment analysis. The analysis used the TFBS matrices available in the JASPAR databases (version Jaspar 2018_NR). Data were visualized through the circos software http://circos.ca/software/.

Statistics and reproducibility

We did not use statistical methods to predetermine sample sizes, but the sample sizes used in this study are similar to or higher than those used in previous studies (Proske *et al*, 2021; Wagner *et al*, 2021). Specific approaches to randomly allocate samples to groups were not used, and the experiments were not performed in a blinded design. No data were excluded from the analysis. Prism (GraphPad version 7) was used for statistical analyses, and the corresponding tests used are listed in the figure legends.

Acknowledgments

We thank Britta Laubenstein and Christiane Sandberg for excellent technical assistance, Maria Leptin and Norbert Perrimon for flies.

Funding

This work was funded by the DFG as part of CRC 1182 and by the CLSM (INST 257/591-1 FUGG). Xiao Niu received funds from the Chinese Scholarship Council and Weifang Medical University, and Leizhi Shi received funds from the Linyi People's Hospital.

References

Adnot S, Lipskaia L, Bernard D (2019) The STATus of STAT3 in Lung Cell Senescence? *Am J Respir Cell Mol Biol* 61: 5–6

Arbouzova NI, Zeidler MP (2006) JAK/STAT signalling in Drosophila: insights into conserved regulatory and cellular functions. *Development* 133: 2605–2616

Bach EA, Ekas LA, Ayala-Camargo A, Flaherty MS, Lee H, Perrimon N, Baeg GH (2007) GFP reporters detect the activation of the Drosophila JAK/STAT pathway in vivo. *Gene Expr Patterns* 7: 323–331

Baligar P, Pokhrel S, Mukhopadhyay A (2016) Experimental Liver Fibrosis and Intrasplenic Transplantation of CD45+ Bone Marrow Cells. *Bio-protocol* 6: e1972

Bosch JA, Tran NH, Hariharan IK (2015) CoinFLP: a system for efficient mosaic screening and for visualizing clonal boundaries in Drosophila. *Development* 142: 597–606

Bossen J, Uliczka K, Steen L, Neugebauer P, Mai MM, Fink C, Stracke F, Heine H, Roeder T (2021) Driver mutations in major lung cancer oncogenes can be analyzed in Drosophila models. *ALTEX* 38: 235–244

Bossen J, Uliczka K, Steen L, Pfefferkorn R, Mai MM, Burkhardt L, Spohn M, Bruchhaus I, Fink C, Heine H *et al* (2019) An EGFR-Induced Drosophila Lung Tumor Model Identifies Alternative Combination Treatments. *Mol Cancer Ther* 18: 1659–1668

Brand AH, Perrimon N (1993) Targeted gene expression as a means of altering cell fates and generating dominant phenotypes. *Development* 118: 401–415

Brown S, Hu N, Hombria JC (2001) Identification of the first invertebrate interleukin JAK/STAT receptor, the Drosophila gene domeless. *Curr Biol* 11: 1700–1705

Campos-Ortega JA, Hartenstein V (1997) *The Embryonic Development of Drosophila melanogaster*. Springer-Verlag Berlin Heidelberg

Chen F, Krasnow MA (2014) Progenitor outgrowth from the niche in Drosophila trachea is guided by FGF from decaying branches. *Science* 343: 186–189

Chen X, Miao M, Zhou M, Chen J, Li D, Zhang L, Sun A, Guan M, Wang Z, Liu P *et al* (2021) Poly-L-arginine promotes asthma angiogenesis through induction of FGFBP1 in airway epithelial cells via activation of the mTORC1-STAT3 pathway. *Cell Death Dis* 12: 761

Choi SM, McAleer JP, Zheng M, Pociask DA, Kaplan MH, Qin S, Reinhart TA, Kolls JK (2013) Innate Stat3-mediated induction of the antimicrobial protein Reg3gamma is required for host defense against MRSA pneumonia. *J Exp Med* 210: 551–561

D'Amico S, Shi J, Martin BL, Crawford HC, Petrenko O, Reich NC (2018) STAT3 is a master regulator of epithelial identity and KRAS-driven tumorigenesis. *Genes Dev* 32: 1175–1187

Daubeuf F, Frossard N (2013) Acute Asthma Models to Ovalbumin in the Mouse. *Curr Protoc Mouse Biol* 3: 31–37

Dutta P, Sabri N, Li J, Li WX (2014) Role of STAT3 in lung cancer. *JAKSTAT* 3: e999503

Fink C, Hoffmann J, Knop M, Li Y, Isermann K, Roeder T (2016) Intestinal FoxO signaling is required to survive oral infection in Drosophila. *Mucosal Immunol* 9: 927–936

Gao H, Guo RF, Speyer CL, Reuben J, Neff TA, Hoesel LM, Riedemann NC, McClintock SD, Sarma JV, Van Rooijen N *et al* (2004) Stat3 activation in acute lung injury. *J Immunol* 172: 7703–7712

Georas SN, Donohue P, Connolly M, Wechsler ME (2021) JAK inhibitors for asthma. *J Allergy Clin Immunol* 148: 953–963

Georas SN, Rezaee F (2014) Epithelial barrier function: at the front line of asthma immunology and allergic airway inflammation. *J Allergy Clin Immunol* 134: 509–520

Glasheen BM, Robbins RM, Piette C, Beitel GJ, Page-McCaw A (2010) A matrix metalloproteinase mediates airway remodeling in Drosophila. *Dev Biol* 344: 772–783

Gon Y, Hashimoto S (2018) Role of airway epithelial barrier dysfunction in pathogenesis of asthma. *Allergol Int* 67: 12–17

Guha A, Lin L, Kornberg TB (2008) Organ renewal and cell divisions by differentiated cells in Drosophila. *Proc Natl Acad Sci U S A* 105: 10832–10836

Harrison DA, Binari R, Nahreini TS, Gilman M, Perrimon N (1995) Activation of a Drosophila Janus kinase (JAK) causes hematopoietic neoplasia and developmental defects. *EMBO J* 14: 2857–2865

Heijink IH, Brandenburg SM, Postma DS, van Oosterhout AJ (2012) Cigarette smoke impairs airway epithelial barrier function and cell-cell contact recovery. *Eur Respir J* 39: 419–428

Hewitt RJ, Lloyd CM (2021) Regulation of immune responses by the airway epithelial cell landscape. *Nature Reviews Immunology* 21: 347–362

Hokuto I, Ikegami M, Yoshida M, Takeda K, Akira S, Perl AK, Hull WM, Wert SE, Whitsett JA (2004) Stat-3 is required for pulmonary homeostasis during hyperoxia. *J Clin Invest* 113: 28–37

Hoskins RA, Carlson JW, Wan KH, Park S, Mendez I, Galle SE, Booth BW, Pfeiffer BD, George RA, Svirskas R *et al* (2015) The Release 6 reference sequence of the Drosophila melanogaster genome. *Genome Res* 25: 445–458

Hu X, Li J, Fu M, Zhao X, Wang W (2021) The JAK/STAT signaling pathway: from bench to clinic. *Signal Transduct Target Ther* 6: 402

Isaac DD, Andrew DJ (1996) Tubulogenesis in Drosophila: a requirement for the trachealess gene product. *Genes Dev* 10: 103–117

Jayaram SA, Senti KA, Tiklova K, Tsarouhas V, Hemphala J, Samakovlis C (2008) COPI vesicle transport is a common requirement for tube expansion in Drosophila. *PLoS One* 3: e1964

Jeon M, Nguyen H, Bahri S, Zinn K (2008) Redundancy and compensation in axon guidance: genetic analysis of the Drosophila Ptp10D/Ptp4E receptor tyrosine phosphatase subfamily. *Neural Dev* 3: 3

Jiang H, Patel PH, Kohlmaier A, Grenley MO, McEwen DG, Edgar BA (2009) Cytokine/Jak/Stat signaling mediates regeneration and homeostasis in the Drosophila midgut. *Cell* 137: 1343–1355

Jin H, Ciechanowicz AK, Kaplan AR, Wang L, Zhang PX, Lu YC, Tobin RE, Tobin BA, Cohn L, Zeiss CJ *et al* (2018) Surfactant protein C dampens inflammation by decreasing JAK/STAT activation during lung repair. *Am J Physiol Lung Cell Mol Physiol* 314: L882–L892

Kallsen K, Zehethofer N, Abdelsadik A, Lindner B, Kabesch M, Heine H, Roeder T (2015) ORMDL deregulation increases stress responses and modulates repair pathways in Drosophila airways. *J Allergy Clin Immunol* 136: 1105–1108

Kida H, Mucenski ML, Thitoff AR, Le Cras TD, Park KS, Ikegami M, Muller W, Whitsett JA (2008) GP130-STAT3 regulates epithelial cell migration and is required for repair of the bronchiolar epithelium. *Am J Pathol* 172: 1542–1554

Kiu H, Nicholson SE (2012) Biology and significance of the JAK/STAT signalling pathways. *Growth Factors* 30: 88–106

Levi BP, Ghabrial AS, Krasnow MA (2006) Drosophila talin and integrin genes are required for maintenance of tracheal terminal branches and luminal organization. *Development* 133: 2383–2393

Levine BD, Cagan RL (2016) Drosophila Lung Cancer Models Identify Trametinib plus Statin as Candidate Therapeutic. *Cell Rep* 14: 1477–1487

Lindsay SA, Lin SJH, Wasserman SA (2018) Short-Form Bomanins Mediate Humoral Immunity in Drosophila. *J Innate Immun* 10: 306–314

Liu L, Johnson WA, Welsh MJ (2003) Drosophila DEG/ENaC pickpocket genes are expressed in the tracheal system, where they may be involved in liquid clearance. *Proc Natl Acad Sci U S A* 100: 2128–2133

Liu RY, Zeng Y, Lei Z, Wang L, Yang H, Liu Z, Zhao J, Zhang HT (2014) JAK/STAT3 signaling is required for TGF-beta-induced epithelial-mesenchymal transition in lung cancer cells. *Int J Oncol* 44: 1643–1651

Lock JG, Stow JL (2005) Rab11 in recycling endosomes regulates the sorting and basolateral transport of E-cadherin. *Mol Biol Cell* 16: 1744–1755

Major J, Crotta S, Llorian M, McCabe TM, Gad HH, Priestnall SL, Hartmann R, Wack A (2020) Type I and III interferons disrupt lung epithelial repair during recovery from viral infection. *Science* 369: 712–717

Makris S, Paulsen M, Johansson C (2017) Type I Interferons as Regulators of Lung Inflammation. *Front Immunol* 8: 259

Martin M (2011) Cutadapt Removes Adapter Sequences From High-Throughput Sequencing Reads. *EMBnetjournal* 17: 10–12

McGuire SE, Mao Z, Davis RL (2004) Spatiotemporal gene expression targeting with the TARGET and gene-switch systems in Drosophila. *Sci STKE* 2004: pl6

Miguel-Aliaga I, Jasper H, Lemaitre B (2018) Anatomy and Physiology of the Digestive Tract of Drosophila melanogaster. *Genetics* 210: 357–396

Milara J, Ballester B, Morell A, Ortiz JL, Escriva J, Fernandez E, Perez-Vizcaino F, Cogolludo A, Pastor E, Artigues E *et al* (2018) JAK2 mediates lung fibrosis, pulmonary vascular remodelling and hypertension in idiopathic pulmonary fibrosis: an experimental study. *Thorax* 73: 519–529

Morris R, Kershaw NJ, Babon JJ (2018) The molecular details of cytokine signaling via the JAK/STAT pathway. *Protein Sci* 27: 1984–2009

Nogueira-Silva C, Santos M, Baptista MJ, Moura RS, Correia-Pinto J (2006) IL-6 is constitutively expressed during lung morphogenesis and enhances fetal lung explant branching. *Pediatr Res* 60: 530–536

Oshima K, Fehon RG (2011) Analysis of protein dynamics within the septate junction reveals a highly stable core protein complex that does not include the basolateral polarity protein Discs large. *J Cell Sci* 124: 2861–2871

Pandey UB, Nichols CD (2011) Human disease models in Drosophila melanogaster and the role of the fly in therapeutic drug discovery. *Pharmacol Rev* 63: 411–436

Parakh S, Ernst M, Poh AR (2021) Multicellular Effects of STAT3 in Non-small Cell Lung Cancer: Mechanistic Insights and Therapeutic Opportunities. *Cancers (Basel)* 13

Paris AJ, Hayer KE, Oved JH, Avgousti DC, Toulmin SA, Zepp JA, Zacharias WJ, Katzen JB, Basil MC, Kremp MM *et al* (2020) STAT3-BDNF-TrkB signalling promotes alveolar epithelial regeneration after lung injury. *Nat Cell Biol* 22: 1197–1210

Perrimon N, Mahowald AP (1986) l(1)hopscotch, A larval-pupal zygotic lethal with a specific maternal effect on segmentation in Drosophila. *Dev Biol* 118: 28–41

Piairo P, Moura RS, Baptista MJ, Correia-Pinto J, Nogueira-Silva C (2018) STATs in Lung Development: Distinct Early and Late Expression, Growth Modulation and Signaling Dysregulation in Congenital Diaphragmatic Hernia. *Cell Physiol Biochem* 45: 1–14

Powers N, Srivastava A (2019) JAK/STAT signaling is involved in air sac primordium development of Drosophila melanogaster. *FEBS Lett* 593: 658–669

Prange R, Thiedmann M, Bhandari A, Mishra N, Sinha A, Hasler R, Rosenstiel P, Uliczka K, Wagner C, Yildirim AO *et al* (2018) A Drosophila model of cigarette smoke induced COPD identifies Nrf2 signaling as an expedient target for intervention. *Aging (Albany NY)* 10: 2122–2135

Prele CM, Yao E, O'Donoghue RJ, Mutsaers SE, Knight DA (2012) STAT3: a central mediator of pulmonary fibrosis? *Proc Am Thorac Soc* 9: 177–182

Proske A, Bossen J, von Frieling J, Roeder T (2021) Low-protein diet applied as part of combination therapy or stand-alone normalizes lifespan and tumor proliferation in a model of intestinal cancer. *Aging (Albany NY)* 13: 24017–24036

Quinton LJ, Mizgerd JP (2011) NF-kappaB and STAT3 signaling hubs for lung innate immunity. *Cell Tissue Res* 343: 153–165

Roeder T, Isermann K, Kabesch M (2009) Drosophila in asthma research. *Am J Respir Crit Care Med* 179: 979–983

Roeder T, Isermann K, Kallsen K, Uliczka K, Wagner C (2012) A Drosophila asthma model - what the fly tells us about inflammatory diseases of the lung. *Adv Exp Med Biol* 710: 37–47

Sato M, Kitada Y, Tabata T (2008) Larval cells become imaginal cells under the control of homothorax prior to metamorphosis in the Drosophila tracheal system. *Dev Biol* 318: 247–257

Simeone-Penney MC, Severgnini M, Tu P, Homer RJ, Mariani TJ, Cohn L, Simon AR (2007) Airway epithelial STAT3 is required for allergic inflammation in a murine model of asthma. *J Immunol* 178: 6191–6199

Tadokoro T, Wang Y, Barak LS, Bai Y, Randell SH, Hogan BL (2014a) IL-6/STAT3 promotes regeneration of airway ciliated cells from basal stem cells. *Proc Natl Acad Sci U S A* 111: E3641–3649

Tadokoro T, Wang Y, Barak LS, Bai Y, Randell SH, Hogan BLM (2014b) IL-6/STAT3 promotes regeneration of airway ciliated cells from basal stem cells. *Proceedings of the National Academy of Sciences* 111: E3641–E3649

Tsarouhas V, Senti KA, Jayaram SA, Tiklova K, Hemphala J, Adler J, Samakovlis C (2007) Sequential pulses of apical epithelial secretion and endocytosis drive airway maturation in Drosophila. *Dev Cell* 13: 214–225

Villarino AV, Kanno Y, O'Shea JJ (2017) Mechanisms and consequences of Jak-STAT signaling in the immune system. *Nat Immunol* 18: 374–384

Wagner C, Uliczka K, Bossen J, Niu X, Fink C, Thiedmann M, Knop M, Vock C, Abdelsadik A, Zissler UM *et al* (2021) Constitutive immune activity promotes JNK- and FoxO-dependent remodeling of Drosophila airways. *Cell Rep* 35: 108956

Weaver M, Krasnow MA (2008) Dual origin of tissue-specific progenitor cells in Drosophila tracheal remodeling. *Science* 321: 1496–1499

Whitsett JA, Alenghat T (2015) Respiratory epithelial cells orchestrate pulmonary innate immunity. *Nature immunology* 16: 27–35

Yew-Booth L, Birrell MA, Lau MS, Baker K, Jones V, Kilty I, Belvisi MG (2015) JAK-STAT pathway activation in COPD. *Eur Respir J* 46: 843–845

Zeidler MP, Bausek N (2013) The Drosophila JAK-STAT pathway. *JAKSTAT* 2: e25353

Zhang X, Yue P, Page BD, Li T, Zhao W, Namanja AT, Paladino D, Zhao J, Chen Y, Gunning PT *et al* (2012) Orally bioavailable small-molecule inhibitor of transcription factor Stat3 regresses human breast and lung cancer xenografts. *Proc Natl Acad Sci U S A* 109: 9623–9628

Zheng XJ, Yang ZX, Dong YJ, Zhang GY, Sun MF, An XK, Pan LH, Zhang SL (2016) Downregulation of leptin inhibits growth and induces apoptosis of lung cancer cells via the Notch and JAK/STAT3 signaling pathways. *Biol Open* 5: 794–800

Table 1: Genes that were highly upregulated in response to *Hop.CA* overexpression.

Name	Maximum group mean	Fold change	FDR p-value
CG16772	11.85	135.44	0
hop	286.06	35.43	0
CG14570	42.21	35.37	0
CG14147	55.31	32.88	0
Hsp70Bb	161.51	29.99	0
Ubx	200.46	23.51	0
pre-mod(mdg4)-I	1.12	18.67	2.22648E-06
IM14	11.46	15.14	3.80132E-07
IM4	26.43	14.97	1.74645E-12

CG14569	1576.88	14.73	0
IM2	7.26	14.47	2.01792E-06
CG5791	1.79	13.80	2.90502E-05
CG9121	3.41	11.54	0
IM1	7.16	10.97	7.52122E-05
CG11413	35.70	10.64	3.44242E-07
CG16710	2.13	10.32	1.72352E-07
CG31960	267.26	10.05	0
CG16789	1.45	9.46	5.58576E-09
CG6034	6.92	8.47	4.7943E-11
Ace	2.06	8.19	0
CG13059	9.90	7.58	1.33893E-06
CG31809	8.64	7.39	0
CG7203	9.41	7.21	8.66989E-09
Vha14-2	2.51	7.05	2.31024E-07
wb	7.35	6.69	0
Drs	8166.47	6.64	0
CG5778	3.20	6.61	0.000294835
CG3457	2.69	6.34	2.38755E-06
Lcp65Ad	9.93	5.79	2.58249E-08
lectin-22C	29.06	5.67	6.88538E-06
fuss	3.97	5.67	0
CG43333	2.39	5.63	1.48392E-09
CG18336	2.96	5.49	5.52167E-05
CG32563	3.06	5.35	0.000696584
FASN2	1.65	5.34	2.95545E-10
Cyp4d21	45.70	5.31	0
Obp57d	1.80	5.28	0.000102926
CG17560	2.31	5.22	0.000766701
CG5888	68.16	5.20	0

$p < 1\times10^{-4}$, fold change > 5, maximum group mean > 1. The list is restricted to 39 genes.

Table 2: Transcription factor-binding site motifs enriched in 41 highly upregulated genes.

Matrix ID	Matrix name	P-value
MA0023.1	dl (var.2)	0.000443261
MA0022.1	dl	0.00407113
MA0532.1	STAT92E	0.00794732

MA0450.1	hkb	0.00811969
MA0197.2	nub	0.0154201
MA0242.1	Bgb::run	0.0371696
MA0204.1	Six4	0.0443521
MA0444.1	CG34031	0.0488169

A total of 133 transcription factor profiles were used.

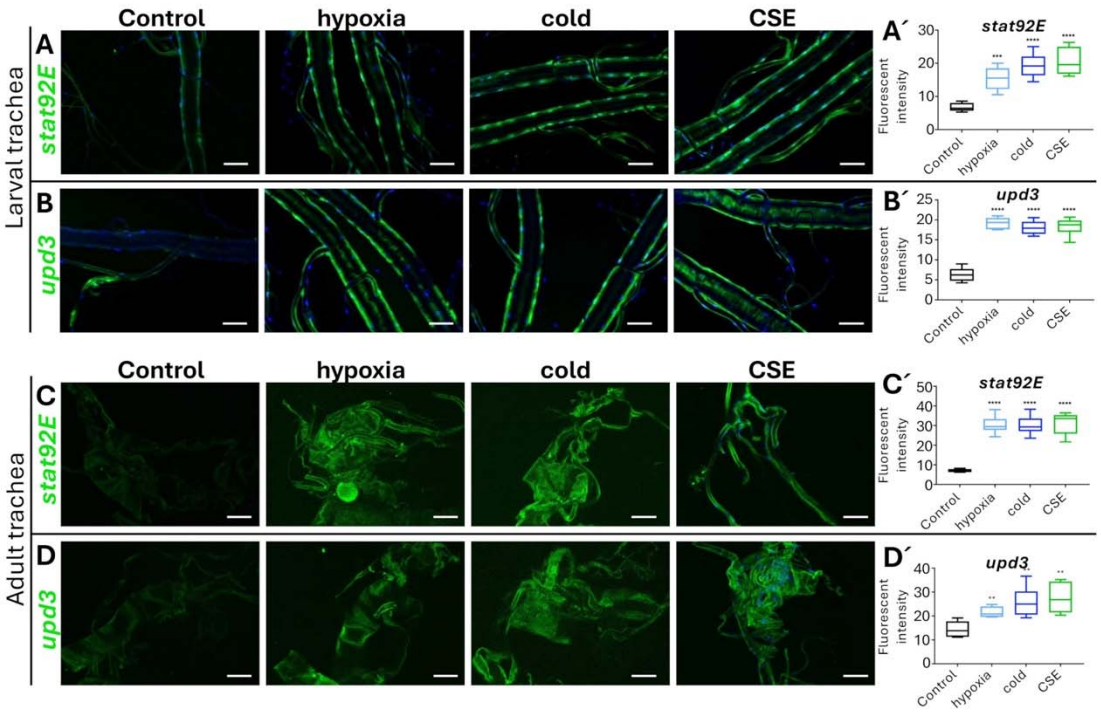

Figure 1: The JAK/STAT signaling pathway in the trachea was activated by external stimuli. (A, C) Fluorescence micrographs of the trachea from *STAT92E-GFP* larvae (A) and adults (C) under control conditions and exposed to external stimuli, which included hypoxia, cold air (cold), and cigarette smoke exposure (CSE). The external stimuli induced the activity of STAT92E, which could be observed and quantified through fluorescent intensity (A' and C'). (B, D) Fluorescence micrographs of the trachea from *upd3-Gal4*; *UAS-GFP* larvae (B) and adults (D) under control conditions and exposed to external stimuli. The expression of *upd3* induced by the external stimuli could be observed and quantified through fluorescent intensity (B' and D'). ** $p < 0.01$, *** $p < 0.001$, **** $p < 0.0001$ by Student's t-test. Scale bar: 100 µm.

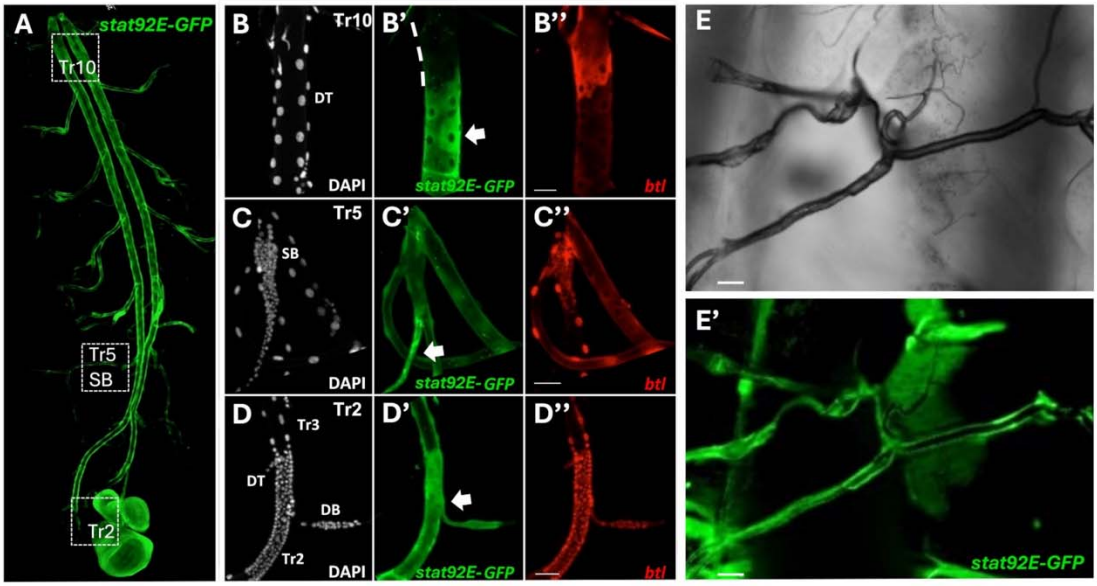

Figure 2: The activation of the JAK/STAT signaling pathway in the respiratory system of *Drosophila*. The activation of the JAK/STAT signaling pathway was detected using a *STAT92E-GFP* reporter, which includes *LacZ* expression under control of *btl-Gal4* (*btl-Gal4*, *STAT92E-GFP*; *UAS-LacZ.nls).* (A-D) STAT92E activity pattern (green) in the larval trachea. JAK/STAT activity is present in most tracheal parts (A). Only the posterior part of the trachea (dorsal trunk (DT) of Tr 10, white dashed line in B) showed decreased JAK/STAT signaling activity (and high *btl* expression; red) compared to other tracheal epithelial cells. Conversely, some regions, like the spiracular branch (SB; C, white arrow) and the dorsal branch (DB) in Tr 2 (D, white arrow), showed increased JAK/STAT signaling activity compared to the tracheal epithelial cells with *btl* expression. (E) STAT92E activity pattern in the adult trachea. Scale bar: 50 µm.

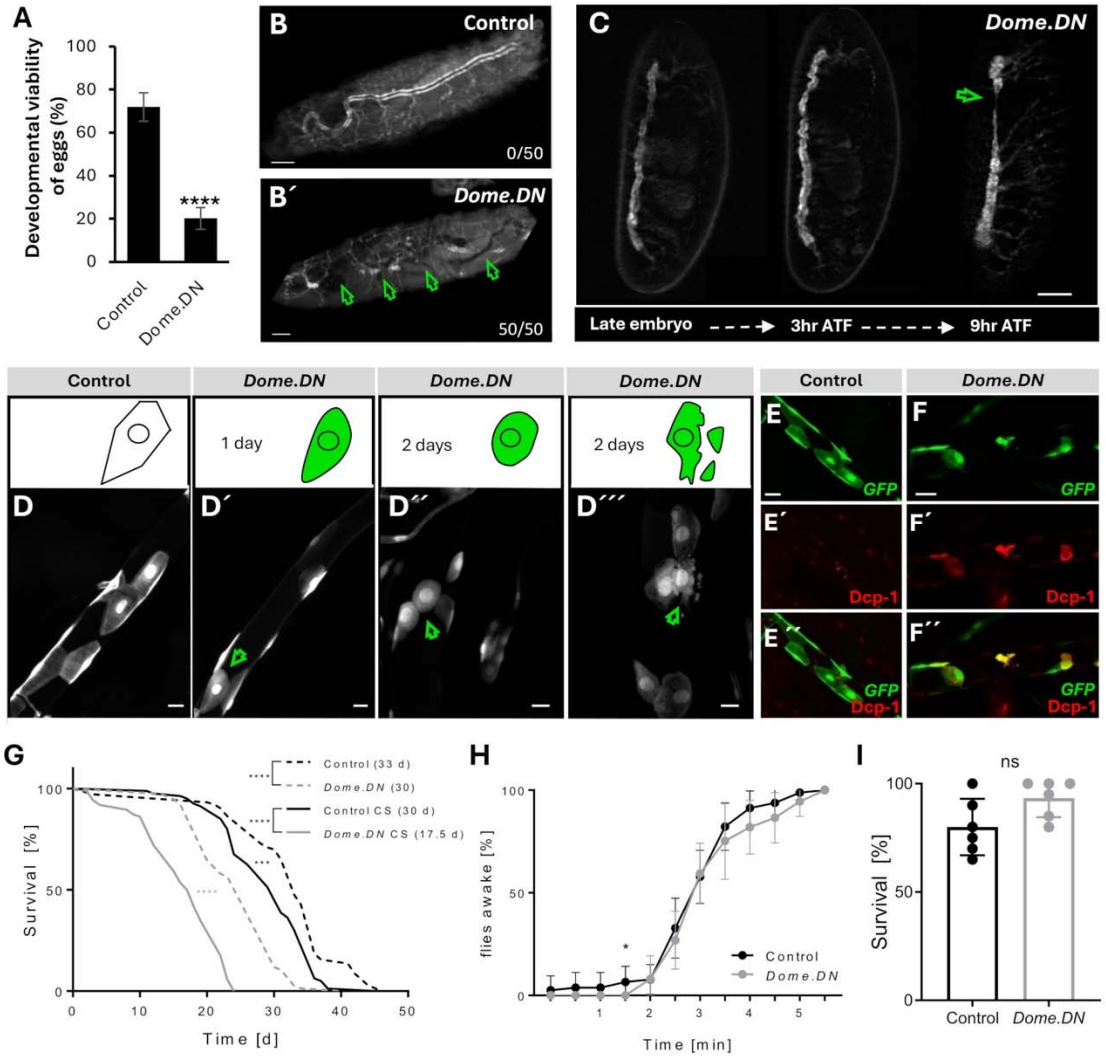

Figure 3: The JAK/STAT signaling pathway inhibition induced epithelial cell apoptosis.

JAK/STAT signaling was blocked in the trachea by expressing *UAS-Dome.DN* under the control of *btl-Gal4;UAS-GFP*. (A) The developmental viability is indicated by the percentage of embryos that hatched. (**** $p < 0.0001$ by Student's t-test). (B) Surviving larvae with tracheal GFP expression. *Dome.DN* expression inhibited the formation of an intact tracheal tree (B'). X/XX: emerged phenotype/total animals. (C) Time-lapse imaging of the trachea of *btl-Gal4>Dome.DN* embryos was conducted continuously for 9 hours after tracheal formation (9hr ATF). Scale bar: 50 µm. (D-F) *Dome.DN* expressing mosaic mutant clones (GFP, green) in the larval trachea (*vvl-FLP*, *CoinFLP-Gal4*, *UAS-EGFP*; *tub-Gal80[ts]* (*vvl-coin.ts*)>*Dome.DN*). (D) Blocking of the JAK/STAT pathway by expressing *Dome.DN* in the trachea led to changes in cell morphology (D' and D'', green arrows) and subsequent disintegration (D''', green

arrow). Scale bar: 20 µm. (E-F) Fluorescence micrographs of the tracheal somatic cells of control *vvl-coin.ts* larvae (E), and the tracheal somatic cells of *vvl-coin.ts>Dome.DN* larvae (F) stained for cleaved Dcp-1 (red, on day 2 after induction). Scale bar: 50 µm. (G) Lifespan analysis under control conditions and cigarette smoke exposure (CS). Median lifespan is indicated in brackets; n=76-103; Log-rank (Mantel-Cox) test. (H, I) Short-term (H; n=6; unpaired t-test) and long-term (I; n=8-9; Mann-Whitney test) hypoxia treatment. * $p < 0.05$, *** $p < 0.001$, **** $p < 0.0001$.

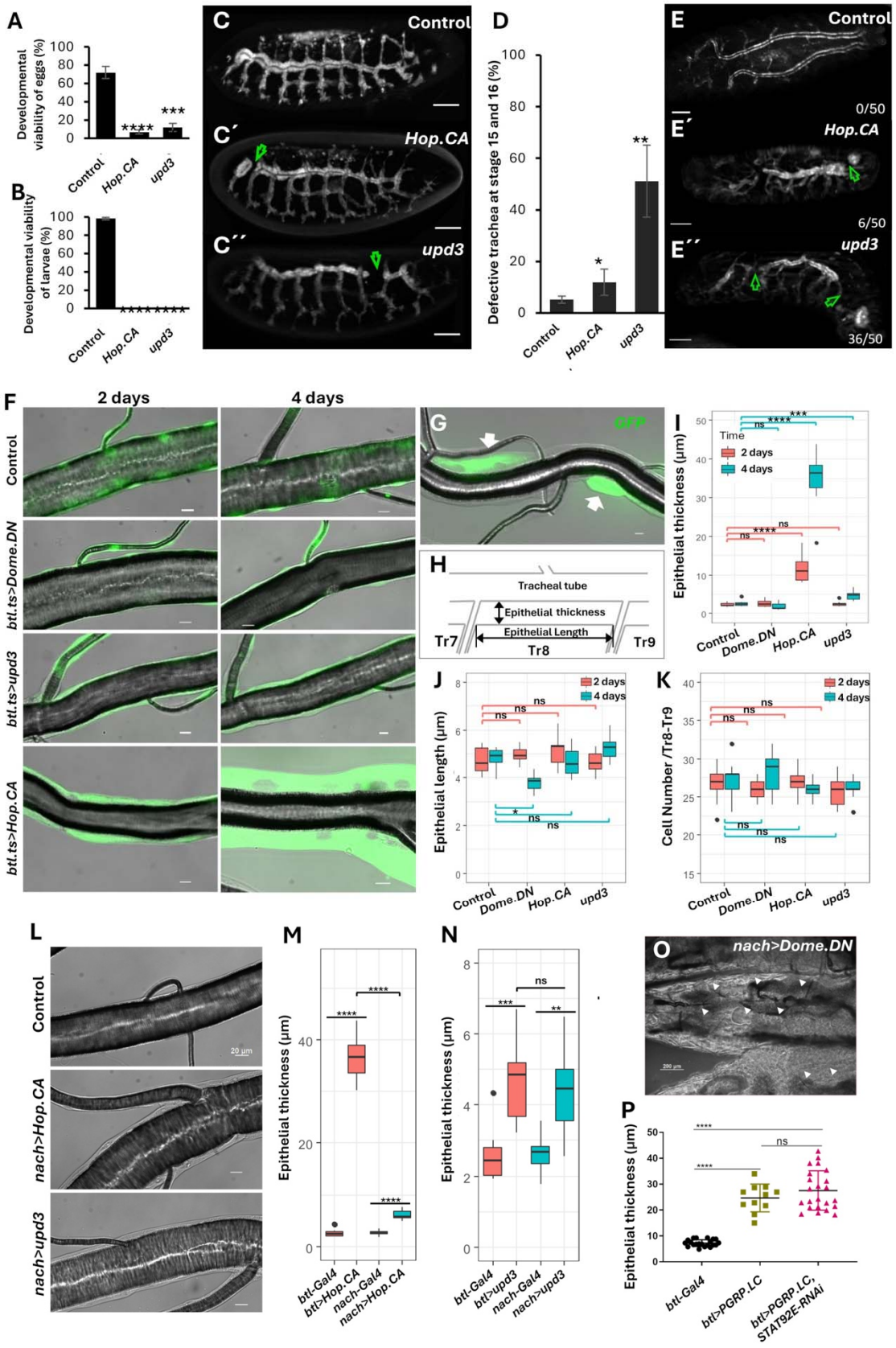
A
Developmental viability of eggs (%)
Control
Hop.CA
upd3
B
Developmental viability of larvae (%)
C
Control
C´
Hop.CA
C´´
upd3
D
Defective trachea at stage 15 and 16 (%)
E
Control
0/50
E´
Hop.CA
6/50
E´´
upd3
36/50
F
2 days
4 days
Control
btl.ts>Dome.DN
btl.ts>upd3
btl.ts>Hop.CA
G
GFP
H
Tracheal tube
Epithelial thickness
Epithelial Length
Tr7
Tr8
Tr9
I
Epithelial thickness (μm)
Time
2 days
4 days
Control
Dome.DN
Hop.CA
upd3
J
Epithelial length (μm)
K
Cell Number /Tr8-Tr9
L
Control
nach>Hop.CA
nach>upd3
M
Epithelial thickness (μm)
btl-Gal4
btl>Hop.CA
nach-Gal4
nach>Hop.CA
N
Epithelial thickness (μm)
btl-Gal4
btl>upd3
nach-Gal4
nach>upd3
O
nach>Dome.DN
P
Epithelial thickness (μm)
btl-Gal4
btl>PGRP.LC
btl>PGRP.LC, STAT92E-RNAi

759

Figure 4: Ectopic JAK/STAT signaling activation in the trachea induced cell thickening. Ectopic activation (*Hop.CA* or *upd3*) or inactivation (*Dome.DN*) of epithelial JAK/STAT signaling. (A-E) Signaling pathway activation during development (*btl>Hop.CA* or *btl>upd3*). (A, B) The percentage of embryos that hatched (A) and the percentage of larvae that developed into pupae (B) are shown. (C) Tracheal GFP expression in embryos. (D-E) Incomplete tracheal development during tracheal morphogenesis. (D) Quantification of the number of defective trachea. (E) Surviving larvae with tracheal GFP expression. Scale bar: 50 µm. (F) Ectopic activation of epithelial JAK/STAT signaling (*Hop.CA* or *upd3*) or inactivation (*Dome.DN*) under control of *btl.ts-Gal4* in the dorsal trunk (DT) of the 8th tracheal metamere (Tr8) of 3rd instar larvae (DT8). Larvae were raised at 29 ℃ for 2 or 4 days for induction of expression, respectively. Scale bar: 20 µm. (G) Micrographs of DT8 of *vvl-FLP*, *CoinFLP-Gal4, UAS-EGFP* (*vvl-coin*)*>Hop.CA* larvae. Scale bar: 20 µm. The thickening of the tracheal epithelium is observed in those cells that express *Hop.CA* (arrows). (H) Illustration of epithelial thickness and epithelial length measurement (arrows). (I-K) Quantification of tracheal epithelial thickness (I), epithelial length (J), and the cell number (K) of larvae with signaling pathway manipulation driven by *btl.ts-Gal4* for 2 or 4 days. (L-O) Mild activation (driven by *nach-Gal4*) of epithelial JAK/STAT (*Hop.CA* or *upd3*) signaling mitigated the thickening phenotype. (L) Micrographs of trachea from larvae with JAK/STAT activation. Scale bar: 20 µm. (M-N) Quantification of the epithelial thickness (DT8). (O) Micrographs of trachea from larvae experiencing suppression of the JAK/STAT pathway (*nach>Dome.DN*). Triangles indicate the tracheal position. Scale bar: 200 µm. (P) Quantification of the epithelial thickness (DT8) of *btl.ts-Gal4*, *btl.ts>PGRP.LC* and *btl.ts>PGRP.LC;STAT92E-RNAi* larvae. Induction of expression in the 3rd instar larval stage for one day. Green arrow: defective region, ns = not significant, * $p < 0.05$, ** $p < 0.01$, *** $p < 0.001$, **** $p < 0.0001$; Student's t-test.

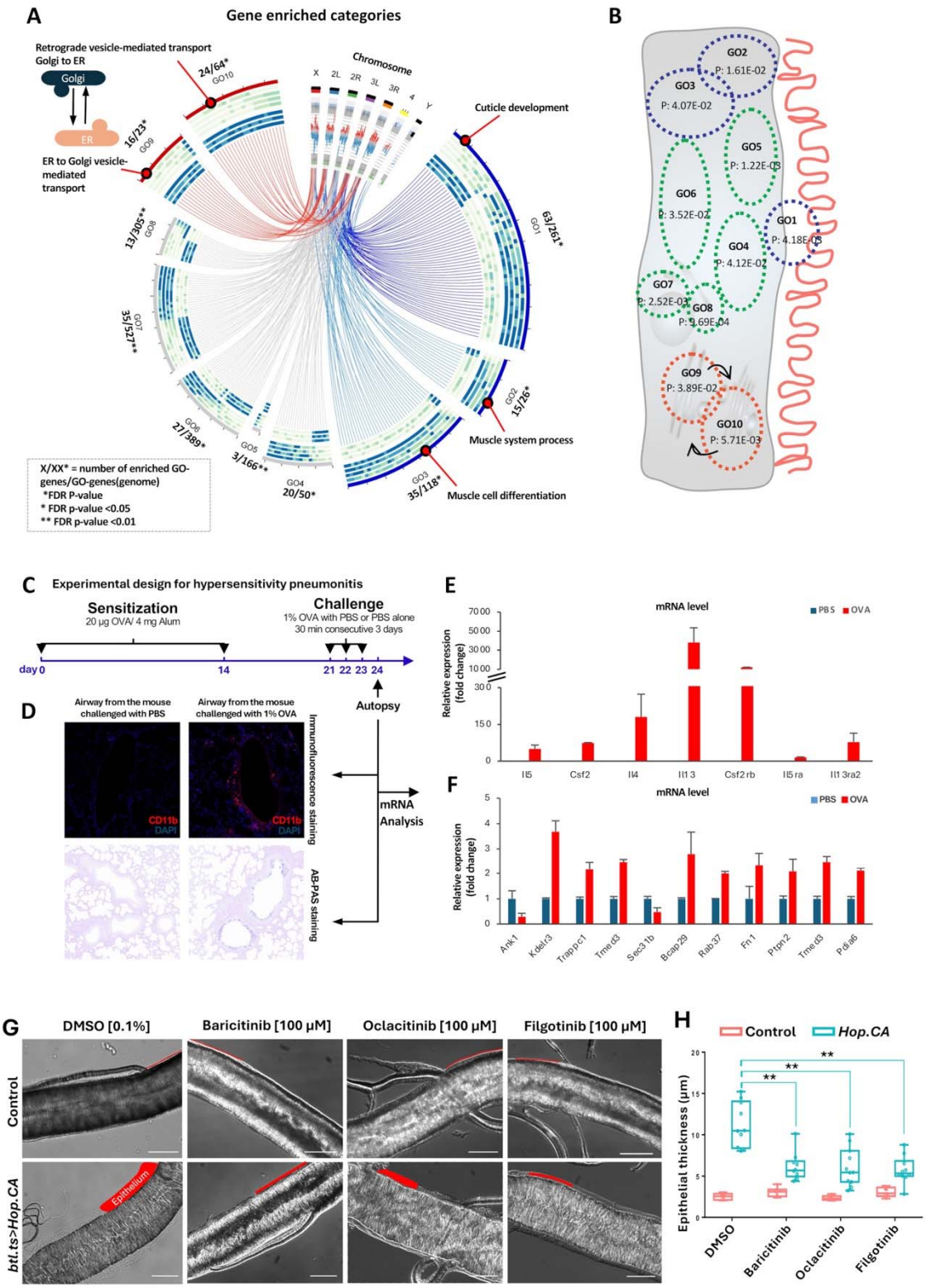

Figure 5: Gene Ontology (GO) enrichment analysis of the 2004 annotated differentially expressed genes in *Hop. CA* overexpressing airways *versus*

controls. (A) Gene ontology (GO) analysis revealed 10 biological processes that were enriched in *Hop.CA* overexpressing airways compared to matching controls. GO1, cuticle development; GO2, muscle system process; GO3, muscle cell differentiation; GO4, glutathione metabolic process; GO5, detection of chemical stimulus; GO6, cellular protein- containing complex assembly; GO7, RNA processing; GO8, translation; GO9, endoplasmic reticulum to Golgi vesicle-mediated transport; GO10, retrograde vesicle-mediated transport from Golgi to the endoplasmic reticulum. Most regulated genes in GO1, GO2, and GO3 were downregulated. Most regulated genes involved in COPI- and COPII-mediated vesicular transport between the endoplasmic reticulum and Golgi (GO9 and GO10) were upregulated. (B) Enriched biological processes were superimposed on a sketch depicting a tracheal epithelial cell, the corresponding *p*-values were included (blue = predominantly downregulated genes; red = predominantly upregulated genes; green = similarly down- and upregulated genes). (C) Experimental design for the OVA- induced asthma model. Mice were sensitized with intraperitoneal injections of 20 µg of OVA emulsified in aluminum hydroxide in a total volume of 1 ml on days 7 and 14, followed by three consecutive challenges each day with exposure to OVA or PBS aerosol for 30 minutes. Mice were sacrificed 24 hours after the final challenge. The left lungs were collected for histological analysis, and the superior lobes were dissected for RNA analysis. (D) The lungs were stained with a CD11b antibody and the standard Alcian blue (AB) method, followed by the Periodic acid–Schiff (PAS) technique. (E) Important chemokines and chemokine receptors induced by OVA aerosol are involved in the JAK/STAT signaling pathway. (F) The genes that function in ER to Golgi vesicle-mediated transport are predominantly upregulated when the mice are exposed to OVA aerosol. (G, H) Changes in tracheal epithelial thickness could be rescued by applying specific JAK inhibitors. (G) Microscopic images of the tracheal epithelium (3rd instar larvae) of Control (*btl.ts>w* ^{1118}) compared to activated JAK/STAT signaling pathway (*btl.ts>Hop.CA*). Scale bar: 50 µm. (H) Quantification of epithelial thickness (highlighted in red) in JAK inhibitor treatment groups compared to the DMSO control. ** $p < 0.01$; Student' s t-test.

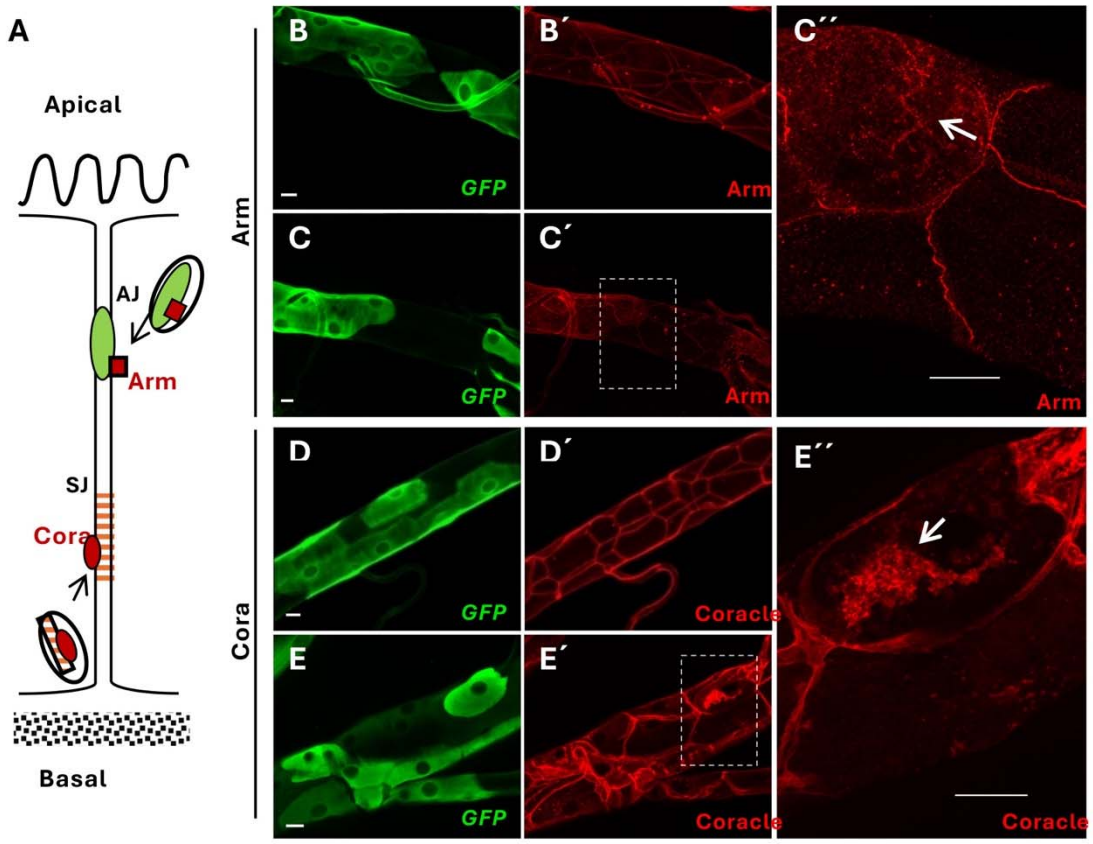

Figure 6: Activation of airway epithelial JAK/STAT signaling affects vesicle-mediated transport of proteins. (A) Schematic orientation of Armadillo (Arm) and Coracle (Cora) at the contact zone between two airway epithelial cells. Adherens junction (AJ), septate junction (SJ). The trachea of *vvl-coin* larvae (control; B and D) and *vvl-coin>Hop.CA* larvae (JAK/STAT activation; C and E) stained for GFP (green, Gal4 positive cells), Arm or Cora (red). Scale bar: 20 µm.

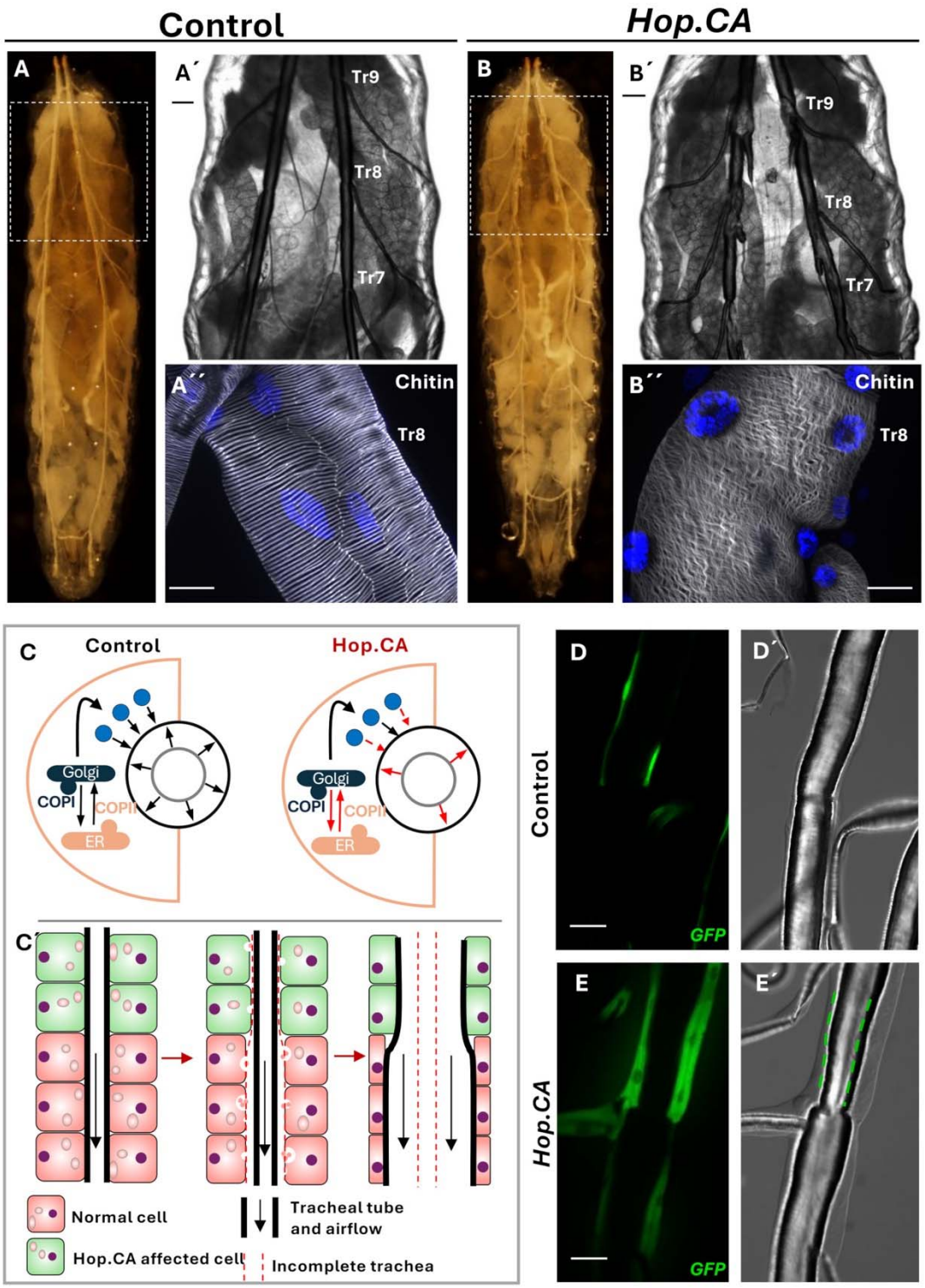

Figure 7: Activation of JAK/STAT signaling in airway epithelial cells affects the development of the epicuticle. (A-B) Activation of JAK/STAT signaling in airway epithelia observed in whole larvae by expressing *Hop.CA* under the control of the *btl.ts* (B-B'') compared to the control (A-A''). (A', B') Magnification of

the posterior larval region. (A'', B'') Chitin staining of isolated airways. (C) Schematic illustration of a potential explanation for the thickening of the epithelium and narrowing of the tube. In the control epithelium, a secretory burst of luminal proteins drives the diametric expansion of the tubes, and this process depends on vesicle-mediated transport. COPI- and COPII-mediated vesicular transport play a central role in this process; mutations in the process underlie the tube size defect in previous reports (Jayaram *et al.*, 2008; Tsarouhas *et al.*, 2007). Although active JAK induced the expression of genes involved in vesicle-mediated transport, long-term activation eventually impedes the transport of vesicles out of the cell (C). This dysfunction in transport could lead to the emergence of tube size defects, such as an increase in cell volume and narrowing of the tube size (C') (Jayaram *et al.*, 2008; Tsarouhas *et al.*, 2007). (D-E) Micrographs of the trachea of *vvl-coin* larvae (control; D) and *vvl-coin>Hop.CA* larvae (E). Cells with *vvl-Gal* expression are stained with GFP (D-E). The green dashed line in E' shows stenosis in the regions with cells expressing *Hop.CA*. Scale bar: 50 µm.